Arctan-Based Robust Droop Control Technique for Accurate Power-Sharing in a Micro-Grid

Marie Aimée Ineza
Department of Electrical Engineering
PAU Institute for Basic Sciences, Technology and Innovation, Nairobi, Kenya
inezamarieaime@gmail.com

Michael Juma Saulo
Department of Electrical and Electronics Engineering, Technical University of Mombasa (TUM), Mombasa, Kenya
michaelsaulo@tum.ac.ke

Cyrus Wabuge Wekesa
School of Engineering
University of Eldoret (UoE)
Eldoret, Kenya
cwekesa@uoeld.ac.ke

Received: 26 December 2021 | Revised: 19 January 2022 | Accepted: 25 January 2022

Abstract-Due to the inherent limitations of the Traditional Droop Controller (TDC), an enhanced droop controller, known as Robust Droop Controller (RDC) has been proposed in previous works. However, this controller cannot compensate for the error in measured frequency, which can potentially contribute to the errors in proper reactive power-sharing as well as degrade frequency regulation. This paper introduces an Arctan-Based Robust Droop Controller (ABRDC) that modifies the RDC for L-inverter to address this issue. The controller, rather than utilizing a linear function, utilizes an arctan-based function for power/frequency droop control. Various simulations were performed in Matlab/Simulink to test the performance of the proposed ABRDC. The results showed that it successfully reduces the frequency error, resulting in improved frequency regulation as well as adequate reactive load power-sharing. The comparative study showed that the ABRDC scheme is more effective than the RDC scheme.

Keywords-parallel-operated inverters; robust droop control; arctan-based function; load power-sharing; frequency and voltage regulation

I. INTRODUCTION

Economic, environmental, and political concerns have increased the attention in Green Energy Generation (GES). The Micro-Grid (MG) concept eases the introduction of GES. Furthermore, it enhances the reliability of distribution networks, minimizes carbon dioxide (CO_2) emissions, transmission losses, etc.. An MG consists of Distributed Generation (DG) sources, storage devices, and loads [1-3]. Power inverters are typically utilized as the link for DG sources, Green Energy Sources (GESs), and storage devices in an MG [4]. They are frequently connected in parallel to increase system reliability and performance and provide high power at a low cost. A vital challenge for parallel-operated inverters in MGs is how to obtain accurate power-sharing amongst them while retaining tight regulation of the MG frequency and voltage magnitude [5]. Droop control is a technique that is often utilized in traditional energy generation systems [6-8]. Its benefit is that there is no requirement for an external communication system between the inverters [5].

When using the Traditional Droop Control (TDC) technique, the inverters operated in parallel ought to have the same per-unit impedance to distribute the load in proportion to their power ratings [9]. The droop controllers ought to produce the same voltage set-point for the inverters as well. In practice, these requirements are challenging to satisfy, resulting in proportionate load power-sharing errors. For this reason, a new approach called Robust Droop Control (RDC) strategy for R-inverters was presented [5] for achieving precise load power-sharing without fulfilling the above two conditions and reducing the voltage drop due to the load droop impact. The method only addressed the power-sharing errors caused by the errors in measuring load voltages. However, this method uses the linear function on the power-frequency droop. The droop based-linear function has a common limitation, the associated output range scaling factor does not affect system dynamics and steady-state condition [10]. If the frequency of the system is calculated using the droop controller based on this linear function, then it can deviate significantly from the nominal value [10, 11]. This results in high frequency errors which can potentially contribute to power-sharing errors, thus leading to inaccuracy in power-sharing amongst parallel operated-inverters and poor frequency regulation.

This work intends to modify the RDC for the L-inverter. Rather than using a linear-based function, it utilizes an arctan based function in power/frequency droop. The idea of using an arctan-based function for the power-frequency droop profile was first presented in [12]. Implementing this arctan-based function offers natural frequency bounds, and enhances the MG's inverter small-signal stability. Thus, incorporating an arctan function into RDC forms a controller that can provide accurate load power-sharing while stabilizing the frequency and PCC voltage regulations at their reference values in the MG of parallel-operated inverters.

A. Limitations of Traditional Droop Control

The form of a droop controller can vary depending on the inverter's output impedance [13-15]. In this work, an inverter of inductive output impedance is considered. Thus, the traditional droop controller is [16]:

$$\begin{cases} w_x = w_n - \alpha_x P_x \\ E_x = E_n - \beta_x Q_x \end{cases} \quad (1)$$

Corresponding author: Marie Aimée Ineza

where P_x and Q_x are the amount of real and reactive power delivered to the bus-bar from each inverter respectively, w_n and w_x are the nominal and output frequencies of the x^{th} inverter, E_n is the nominal voltage, E_x is the RMS value of the reference voltage of the x^{th} inverter V_{refx}, and β_x and α_x are the voltage and frequency droop coefficients respectively. Figure 1 illustrates the TDC diagram.

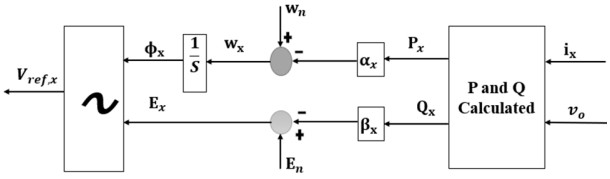

Fig. 1. Traditional droop control diagram.

When the MG is equipped with the TDC in a steady-state condition, the two inverters work at the same frequency, i.e. $w_1 = w_2$ and the relationship in (2) is satisfied. This ensures the active power-sharing accuracy for L-inverters [17] (or reactive power-sharing accuracy for R- inverters [5]).

$$\alpha_1 P_1 = \alpha_2 P_2 \quad (2)$$

In addition, the proportional reactive power for the L-inverters can be achieved when the relationship in (4) is satisfied. However, because of the presence of noise, disturbances, errors, and line impedance mismatches in the MG, the expressions in (3) are practically hard to satisfy [17].

$$\begin{cases} E_1 = E_2 \\ \frac{\beta_1}{X_{01}} = \frac{\beta_2}{X_{02}} \end{cases} \quad (3)$$

B. Limitations of Robust Droop Control

Due to the inherent restrictions when utilizing the TDC for the MG-based inverters, the RDC was proposed in [5] to improve the accuracy of load power-sharing and voltage regulation. As presented in Figure 2, the RDC of the L-inverter is:

$$w_x = w_n - \alpha_x P_x \quad (4)$$

$$\dot{E_x} = \mu(E_n - V_0) - \beta_x Q_x \quad (5)$$

where μ and V_0 are an amplifier and the RMS measured value of the output voltage v_0. At the steady-state condition, (5) becomes:

$$\beta_x Q_x = \mu(E_n - V_0) \quad (6)$$

As long as μ is the same, the right part of (6) is always the same for all parallel-operated inverters [4]. Thus:

$$\beta_x Q_x = \text{constant} \quad (7)$$

which ensures accurate reactive power-sharing without using the same E_x. Therefore, the accuracy of reactive power-sharing is no longer dependent on the output impedance of the inverter and is also resistant to disturbances and errors [4]. However, this method did not compensate for the frequency errors, potentially contributing to load-sharing errors and degradation of frequency regulation.

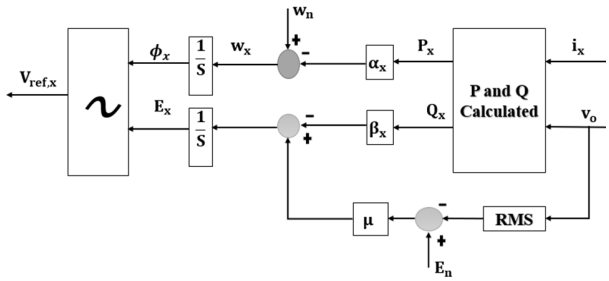

Fig. 2. Robust droop control diagram.

II. THE PROPOSED DROOP CONTROL STRATEGY

A. Design of the Proposed Droop Controller

The proposed Arctan-Based Robust Droop Control (ABRDC) strategy adopts the structure of RDC for L-inverter [5] and utilizes an arctan-based function in power frequency droop control rather than the linear function [18]. This controller gains the benefits of the two methods. This means that the RDC is responsible for eliminating the effect of line impedance mismatches, noise, disturbances, and sharing errors caused by the errors in measuring the load voltage, whereas the arctan-based droop control is responsible for removing the frequency error since a MG-based inverter equipped with arctan droop controller provides naturally frequency boundaries [10, 12]. As a result, the proposed controller is able to provide accurate load power-sharing while ensuring a tight voltage and frequency regulation. Therefore, the P/f of the proposed droop controller is based on the arctan function, and can be expressed as:

$$f_x = f_n - \frac{c_p}{\pi} * arctan\left(\rho\left(P_x - P_{ref}\right)\right) \quad (8)$$

or, as:

$$w_x = w_n - 2c_p * arctan\left(\rho\left(P_x - P_{ref}\right)\right) \quad (9)$$

The Q/E of the proposed droop controller is based on the RDC methodology and it can be expressed as:

$$\dot{E_x} = \mu(E_n - V_0) - \beta_x Q_x \quad (10)$$

where c_p is the multiplier, ρ is the coefficient, P_{ref} is the actual power reference which is always equal to zero in the islanded MG, and the other parameters have already been specified. Referring to (9) and (10), the proposed droop control diagram is illustrated in Figure 3.

The arctan-based function is inherently constrained in the frequency domain from $\left(f_r + \frac{c_p}{2}\right)$ to $\left(f_r - \frac{c_p}{2}\right)$ Hz, which is one of the benefits of this method [12]. The multiplier c_p is mostly set to be 1 to keep the frequency within the limits of 50±0.5H. Additionally, changing the multiplier directly affects the frequency variation boundaries due to the arctan function. As illustrated in Figure 4, as the arctan bounding multiplier increases, the frequency variation increases [19]. Furthermore, the coefficient ρ is used to control the concavity (and inherently over the gradient). The variation in real power may be imposed due to this coefficient, as shown in Figure 5 [19].

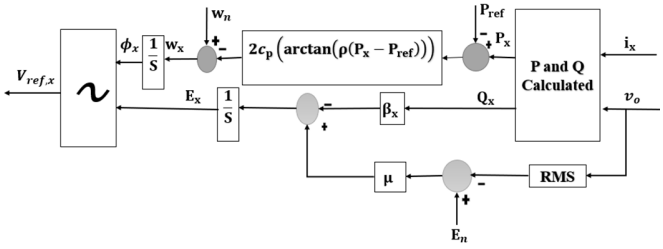

Fig. 3. Proposed droop control diagram.

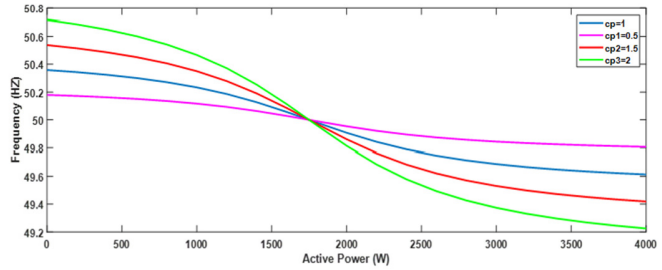

Fig. 4. The impact of variation of the arctan bounding multiplier, c_p [19].

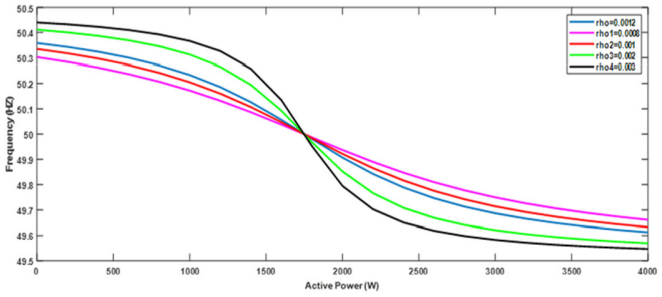

Fig. 5. The impact of variation of the arctan droop coefficient ρ [19].

The output voltage of the x^{th} inverter can be expressed as:

$$V_0 = E_n - \frac{\beta_x}{\mu E_n} E_n \quad (11)$$

which can be kept within the predetermined range through selecting a big value of μ. The proposed control strategy has excellent voltage regulation capability in addition to accurate power-sharing and excellent frequency regulation capability. Figure 6 presents the schematic diagram of the proposed droop controller in MG of one DG unit. Real (P) and reactive (Q) power are computed utilizing the dq transformation for the 3ϕ current and voltage quantities. Based on the computed power flux, the frequency is controlled using the arctan droop control algorithm, whereas the voltage is controlled using the RDC. The inverter's current and voltage outputs are stabilized utilising a cascaded system of the outer voltage and inner current control loops [19, 20]. A Proportional Integral (PI) controller is deployed to reduce the current error with quicker dynamic response and to ensure zero steady-state error [16, 21-23]. It is also utilized to force the calculated q-axis voltage component to be zero and the calculated d-axis voltage component to be equal to the reference value [20].

B. Performance Comparison Criteria of Droop Control Strategies

1) Power-Sharing Ratio Criterion

The load power-sharing ratio criterion is generally used to compare the capability of different droop control methodologies. If the relationship between the power and the droop coefficients of any two DGs in (12) is accomplished, proportionate power-sharing between parallel-operated inverters is acquired.

$$\begin{cases} \frac{\alpha_1}{\alpha_2} = \frac{P_2}{P_1} = \cdots = \frac{\alpha_x}{\alpha_{x+1}} = \frac{P_{x+1}}{P_x} \\ \frac{\beta_1}{\beta_2} = \frac{Q_2}{Q_1} = \cdots = \frac{\beta_x}{\beta_{x+1}} = \frac{Q_{x+1}}{Q_x} \end{cases} \quad (12)$$

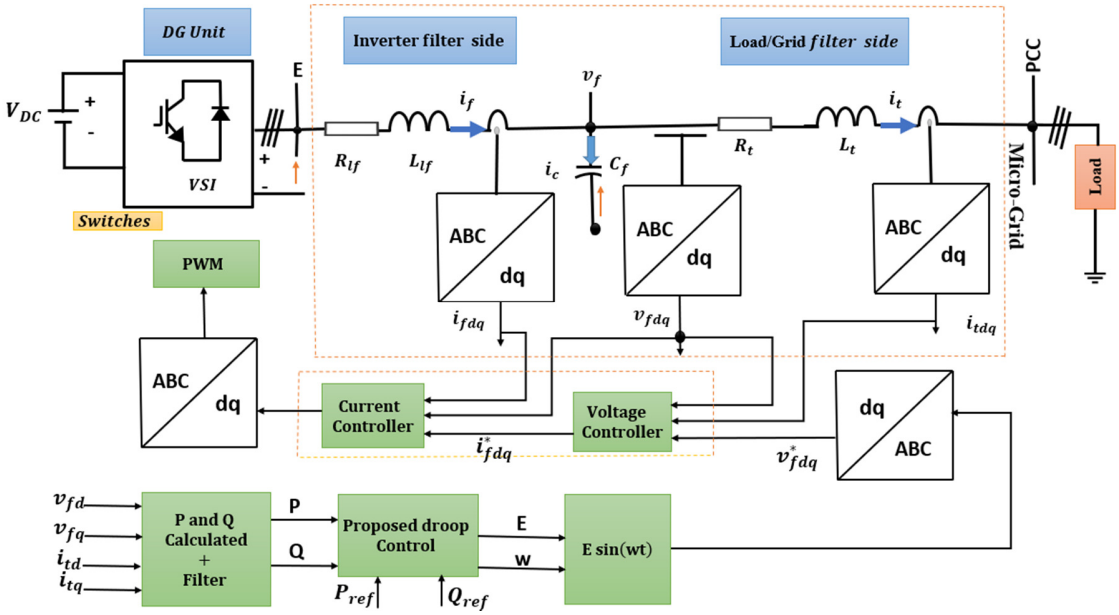

Fig. 6. Schematic diagram of the proposed droop control in one DG unit MG.

2) Power-Sharing Ratio Criterion

Apart from the load power-sharing ratio criterion, the load power-sharing error is also used to analyze and evaluate the capability of droop control techniques. Low error values represent the ability of the control strategy to reduce the load power-sharing imbalances between the inverters, while large values represent a higher imbalance of load power-sharing among the inverters operated in parallel. The real and reactive load power-sharing errors are assessed based on (13):

$$\begin{cases} e_{px} = \frac{P_x^* - P_x}{P_x^*} \times 100 \\ e_{qx} = \frac{Q_x^* - Q_x}{Q_x^*} \times 100 \end{cases} \quad (13)$$

where e_{px} and e_{ax} are the active and reactive load power-sharing errors of the x^{th} inverter in percentage respectively, P_x^* and Q_x^* are the active and reactive power supplied by the x^{th} inverter when the active and reactive power-sharing is in exact proportion to their ratings, and P_x and Q_x are the measured real and reactive power supplied by the x^{th} inverter.

III. SIMULATED RESULTS AND DISCUSSION

A. Simulation Setup

The performance of the developed droop control strategy is evaluated in a MG-based inverter. All models were created using the Matlab/Simulink toolbox. Figures 7-8 depict the Simulink model of the proposed droop controller in a stand-alone MG of two parallel-operated inverters and all submodels. Table I shows the system parameters used during the simulations. Table II summarizes the investigated scenarios.

TABLE I. SYSTEM PARAMETERS

Parameter	Value
Nominal voltage	E_n =400 V
DC bus voltage	V_{dc} =850 V
Nominal frequency	f_n =50 Hz
Inverter switching time	$T_{s\,inverter}$ =5 KHz
Load1	$Q_{L1} = 3e^3$ Var, $P_{L1} = 6e^3$ W
Load2	$Q_{L2} = 3e^3$ Var, $P_{L2} = 6e^3$ W
Line$_1$ impedance	$R_{L1} = 0.7\,\Omega$, $L_{L1} = 0.005$ H
Line$_2$ impedance	$R_{L2} = 0.8\Omega$, $L_{L2} = 0.006$ H
Filter	$C_{f1} = C_{f2} = 2.5e^{-4}$ F, $L_{f1} = L_{f2} = 2e^{-3}$ H
Voltage and frequency droop coefficients	$\beta_1 = \beta_2 = 2.5e^{-5}$ V/Var $\alpha_1 = \alpha_2 = 6.25e^{-5}$ rad/SW
Arctan bounding multiplier	$c_{p1} = c_{p2} = 1$ HZ/W
Arctan droop coefficient	$\rho_1 = \rho_2 = 1e^{-5}$ rad/S.W.
Amplifier	$\mu_1 = \mu_2$ =2
Inner loops PI coefficients	$K_{pi} = 0.15$, $K_{ii} = 1.5$, $K_{pv} = 20$, $K_{iv} = 1000$.

TABLE II. OPERATION SCENARIOS

Time (s)	Operation
0-6	Two DGs unit powers the load.
6-12	Load 2 is added to the system
12-18	Load 2 is removed from the system

B. Frequency and Voltage Stability Analysis

Figures 9-10 present the frequency and PCC voltage stability when the ABRDC technique is adopted. It can be seen that the ABRDC can maintain the frequency and output PCC voltage during the steady-state condition to their reference values of 50HZ and 400V. At the time *t*=6s, load 2 was added to the system and the frequency and output PCC voltage dropped from 50 to 49.99HZ and from 400V to 396.10V respectively. At *t*=12s, load 2 was disconnected from the system and frequency and PCC voltage were reset to their previous values. As observed, the ABRDC technique can retain the voltage and frequency at their reference values during the steady-state condition. It can also keep the voltage and frequency deviations within the allowed range according to IEEE1547-2018 standards (the allowable range for frequency and voltage variation are ±1% and ±5% of the given reference values respectively) when a load change is added to the system.

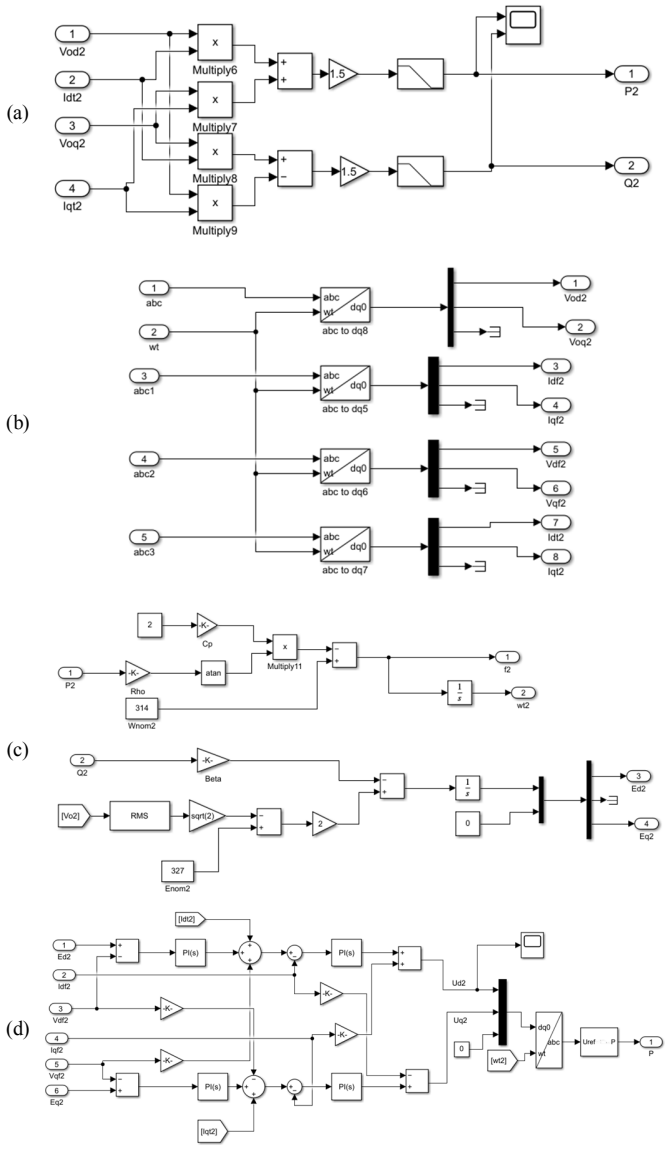

Fig. 7. SIMULINK submodel of : (a) P&Q calculated, (b) abc to dqo transformation, (c) proposed droop controller, (d) cascade control loop.

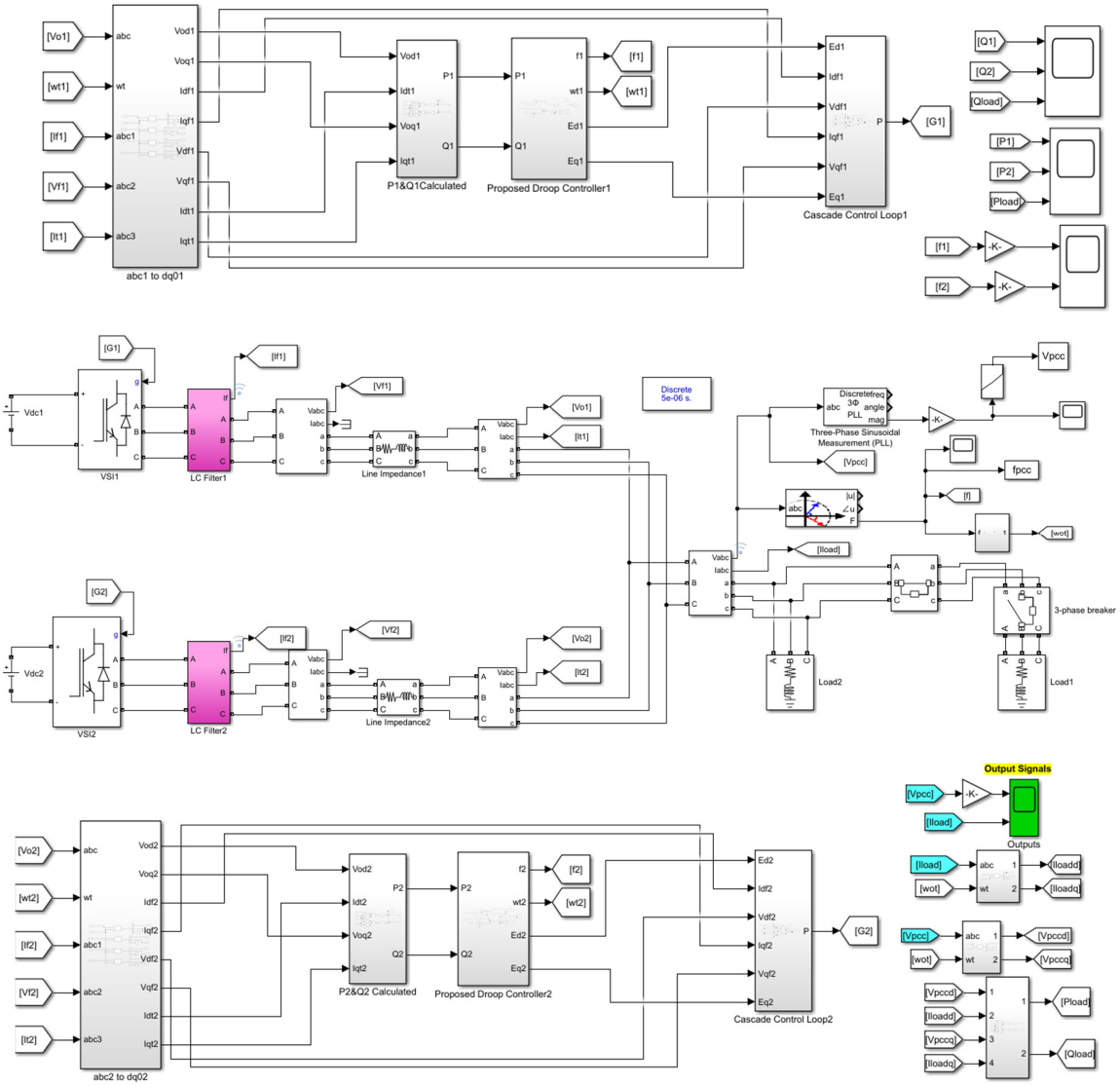

Fig. 8. SIMULINK model of the proposed droop controller in a stand-alone MG of two parallel-operated inverters.

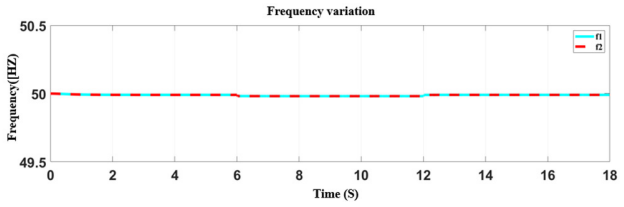

Fig. 9. Frequency variation for inverters using the proposed droop controller.

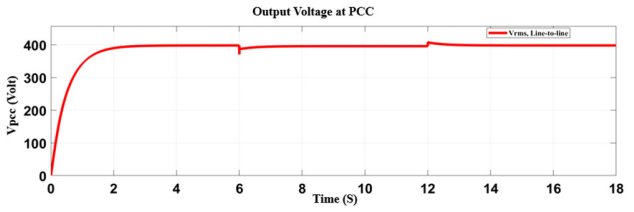

Fig. 10. Voltage regulation at PCC using the proposed droop controller.

C. Active and Reactive Power-Sharing Analysis

The load power-sharing capability of the ABRDC in an MG of two parallel-operated inverters is also analyzed in this study. As depicted in Figures 11-12, during the steady-state condition, the active and reactive load powers were correctly shared with ratios of α_1: α_2=P_1:P_2=3e^{3}W:3e^{3}W and β_1:β_2=1:1=Q_1:Q_2=1.5e^3 Var:1.5e^3 Var respectively. Load 2 was introduced to the system at t=6-12s to verify the controller's performance as the load in the MG increases. The inverters kept distributing the active and reactive load power in a proportional manner, where the ratios were α_1:α_2=P_1:P_2=6e^{3}W:6e^{3}W for the real power and β_1:β_2=1:1=Q_1:Q_2=3e^{3}Var:3e^{3}Var for the reactive power. At t=12-18s, load 2 was disconnected from the system, the active and reactive power were also appropriately distributed, and the ratios were α_1:α_2=1:1=P_1:P_2=3e^{3}W:3e^{3}W and β_1:β_2=1:1 =Q_1:Q_2=1.5e^{3}Var:1.5e^{3}Var respectively. As seen, the ABRDC technique satisfies the conditions of the load power-sharing in all scenarios, thus it ensures accurate power-sharing.

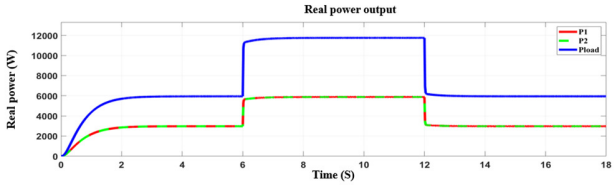

Fig. 11. The real power-sharing amongst two inverters operated in parallel utilizing the proposed controller.

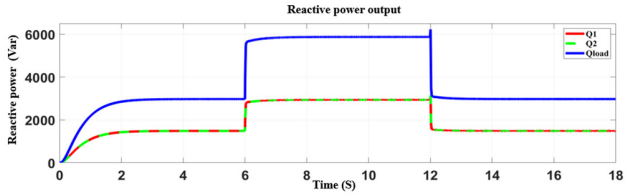

Fig. 12. The reactive power-sharing amongst two inverters operated in parallel utilizing the proposed controller.

D. Comparative Study Analysis between the Proposed and Robust Droop Control Techniques

To validate the proposed droop control methodology, comparative analysis of the ABRDC and RDC methodologies based on the frequency variation for the inverter, voltage regulation at PCC, and the active and reactive load power-sharing amongst the inverters operating in parallel was performed. The frequency variation comparison of the two controllers is presented in Figure 13. As seen, during the steady-state condition at t=0-6s, the ABRDC technique can retain the frequency at the reference value of 50HZ, whereas it drops to 49.81HZ for the RDC. In Figure 14, the voltage regulation at PCC when utilising ABRDC and RDC techniques is compared. Both ABRDC and RDC techniques could regulate the output voltage at PCC to the reference value of 400V. At t=6-12s, load 2 was added to the system. The frequency decreases from 50 to 49.99HZ for ABRDC and from 49.81 to 49.63HZ for RDC. The output voltage at PCC drops to 396.1V for both ABRDC and RDC techniques. When the load 2 is removed from the system, the frequency is restored to 50HZ for the ABRDC technique, while for the RDC technique it was reset to its previous value. Again, the output voltage at PCC was also restored to its reference value for both ABRDC and RDC techniques. In brief, the ABRDC provides better frequency and voltage regulation of 0.02% and 0.45%, respectively, whereas RDC has 0.36% and 0.45% respectively. As demonstrated, the ABRDC technique reduced successfully the frequency error, leading to improved reactive load power-sharing.

The active power-sharing comparison between ABRDC and RDC is presented in Figure 15. It is noted that for all techniques, the real power-sharing ratio is P_1:P_2=1:1, which means each inverter delivers 50% of the total real power of the load in both cases. The reactive power-sharing comparison is seen in Figure 16. The reactive load power-sharing when utilizing the ABRDC technique is enhanced, where VSI_1 supplied 49.98%, and VSI_2 delivered 49.98% of the total reactive power of the load, whereas adopting RDC technique it is 52.48% and 47.52%. This enhancement in reactive load power-sharing when utilizing the proposed controller is due to its capability to reduce the system's frequency error.

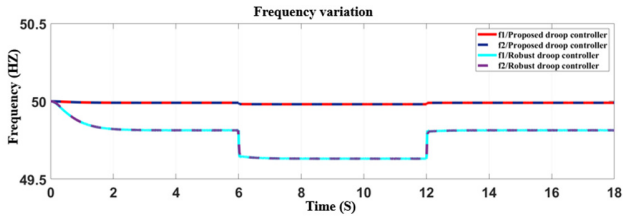

Fig. 13. Comparative analysis of the frequency variation for ABRDC and RDC techniques.

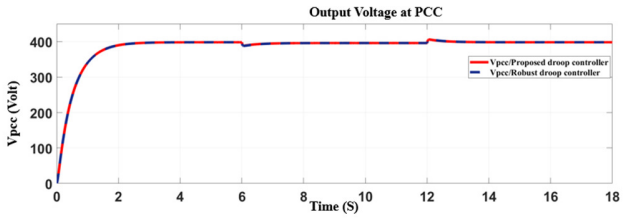

Fig. 14. Comparative analysis of the voltage regulation at PCC using ABRDC and RDC techniques.

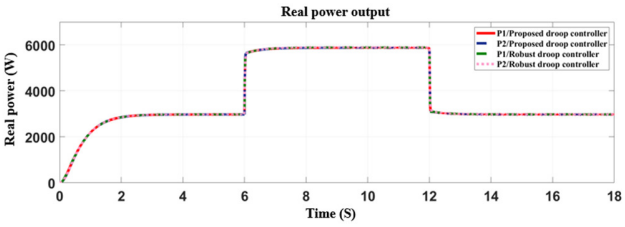

Fig. 15. Comparative analysis of the real power-sharing using ABRDC and RDC techniques.

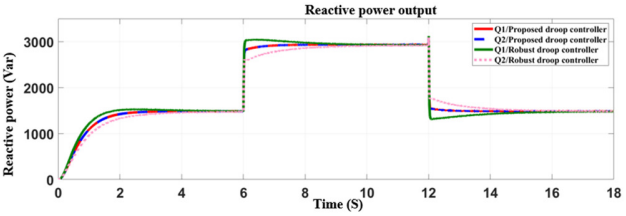

Fig. 16. Comparative analysis of the reactive power-sharing using ABRDC and RDC techniques.

TABLE III. POWER ERRORS

	Active and reactive load power-sharing errors			
Control strategy	e_{P1}(%)	e_{P2}(%)	e_{Q1}(%)	e_{Q2}(%)
ABRDC	0.04	0.09	0.64	0.76
RDC	0.05	0.10	-2.51	4.12

Based on the power-sharing error criterion, a comparative study was performed to assess and analyze the capability and effectiveness of the proposed ABRDC and the RDC. It is noted that the proposed droop controller minimizes power-sharing errors when compared to the RDC, resulting in improved power-sharing. Table III presents the active and reactive load power-sharing errors for the two strategies.

IV. CONCLUSION

This paper proposes the arctan-based robust droop controller (ABRDC) to provide tight frequency and voltage regulations as well as accurate load power-sharing amongst inverters operated in parallel. The proposed controller modifies the structure of the RDC for L-inverters. Rather than using a linear function, it utilizes an arctan based function in power/frequency droop control. This means that the proposed controller gains the benefits of both controllers. The RDC is responsible for mitigating the impact of line impedance mismatches and for reducing the power-sharing errors due to the errors in the measured load voltage. At the same time, the arctan-based function is responsible for minimizing the frequency errors when the load change occurs in the MG. Through various simulations, results showed that the developed droop controller provides accurate load power-sharing while stabilizing the frequency and PCC voltage at the reference values. Furthermore, a comparative study demonstrated that the proposed droop control has more capability and effectiveness than the RDC strategy.

ACKNOWLEDGMENT

The authors acknowledge Pan African University's Institute for Basic Sciences, Technology, and Innovation for funding this research.

REFERENCES

[1] R. H. Lasseter, "Smart Distribution: Coupled Microgrids," *Proceedings of the IEEE*, vol. 99, no. 6, pp. 1074–1082, Jun. 2011, https://doi.org/10.1109/JPROC.2011.2114630.

[2] T. Qunais, "Impacts Analysis of Cross-Coupling Droop Terms on Power Systems with Converter-Based Distributed Energy Resources," Ph.D. dissertation, Mississippi State University, Mississippi State, MS, USA, 2019.

[3] E. Pathan, A. Abu Bakar, S. A. Zulkifi, M. H. Khan, H. Arshad, and M. Asad, "A Robust Frequency Controller based on Linear Matrix Inequality for a Parallel Islanded Microgrid," *Engineering, Technology & Applied Science Research*, vol. 10, no. 5, pp. 6264–6269, 2020, https://doi.org/10.48084/etasr.3769.

[4] Q.-C. Zhong, F. Blaabjerg, J. M. Guerrero, and T. Hornik, "Reduction of voltage harmonics for parallel-operated inverters," in *2011 IEEE Energy Conversion Congress and Exposition*, Phoenix, AZ, USA, Sep. 2011, pp. 473–478, https://doi.org/10.1109/ECCE.2011.6063807.

[5] Q.-C. Zhong, "Robust Droop Controller for Accurate Proportional Load Sharing Among Inverters Operated in Parallel," *IEEE Transactions on Industrial Electronics*, vol. 60, no. 4, pp. 1281–1290, Apr. 2013, https://doi.org/10.1109/TIE.2011.2146221.

[6] R. Majumder, B. Chaudhuri, A. Ghosh, R. Majumder, G. Ledwich, and F. Zare, "Improvement of Stability and Load Sharing in an Autonomous Microgrid Using Supplementary Droop Control Loop," *IEEE Transactions on Power Systems*, vol. 25, no. 2, pp. 796–808, Feb. 2010, https://doi.org/10.1109/TPWRS.2009.2032049.

[7] G. Diaz, C. Gonzalez-Moran, J. Gomez-Aleixandre, and A. Diez, "Scheduling of Droop Coefficients for Frequency and Voltage Regulation in Isolated Microgrids," *IEEE Transactions on Power Systems*, vol. 25, no. 1, pp. 489–496, Oct. 2010, https://doi.org/10.1109/TPWRS.2009.2030425.

[8] P. S. Prasad, A. M. Parimi, and L. Renuka, "Chapter 7 - Control of hybrid AC/DC microgrids," in *Microgrids*, J. M. Guerrero and R. Kandari, Eds. Academic Press, 2022, pp. 191–225, https://doi.org/10.1016/j.rser.2017.03.028.

[9] Q. C. Zhong and T. Hornik, *Control of Power Inverters in Renewable Energy and Smart Grid Integration*. Hoboken, NJ, USA: Wiley-IEEE Press, 2012.

[10] J. D. D. Iyakaremye, G. N. Nyakoe, and C. W. Wekesa, "MPC-Based Arctan Droop Control Strategy of the Parallel Inverter System in an Islanded AC Microgrid," *Journal of Engineering*, vol. 2021, Mar. 2021, Art. no. e1870590, https://doi.org/10.1155/2021/1870590.

[11] K. Manjunath and V. Sarkar, "Performance assessment of different droop control techniques in an AC microgrid," in *2017 7th International Conference on Power Systems (ICPS)*, Pune, India, Sep. 2017, pp. 93–98, https://doi.org/10.1109/ICPES.2017.8387274.

[12] C. N. Rowe, T. J. Summers, R. E. Betz, D. J. Cornforth, and T. G. Moore, "Arctan power-frequency droop for improved microgrid stability," *IEEE Transactions on Power Electronics*, vol. 28, no. 8, pp. 3747–3759, 2013, https://doi.org/10.1109/TPEL.2012.2230190.

[13] Q.-C. Zhong and Y. Zeng, "Parallel operation of inverters with different types of output impedance," in *IECON 2013 - 39th Annual Conference of the IEEE Industrial Electronics Society*, Vienna, Austria, Aug. 2013, pp. 1398–1403, https://doi.org/10.1109/IECON.2013.6699337.

[14] Y. Zeng and Q.-C. Zhong, "A droop controller achieving proportional power sharing without output voltage amplitude or frequency deviation," in *2014 IEEE Energy Conversion Congress and Exposition (ECCE)*, Pittsburgh, PA, USA, Sep. 2014, pp. 2322–2327, https://doi.org/10.1109/ECCE.2014.6953713.

[15] Q. C. Zhong and Y. Zeng, "Universal Droop Control of Inverters with Different Types of Output Impedance," *IEEE Access*, vol. 4, no. 3, pp. 702–712, 2016, https://doi.org/10.1109/ACCESS.2016.2526616.

[16] E. Pathan, S. A. Zulkifli, U. B. Tayab, and R. Jackson, "Small Signal Modeling of Inverter-based Grid-Connected Microgrid to Determine the Zero-Pole Drift Control with Dynamic Power Sharing Controller," *Engineering, Technology & Applied Science Research*, vol. 9, no. 1, pp. 3790–3795, 2019, https://doi.org/10.48084/etasr.2465.

[17] Z. Shuai, S. Mo, J. Wang, Z. J. Shen, W. Tian, and Y. Feng, "Droop control method for load share and voltage regulation in high-voltage microgrids," *Journal of Modern Power Systems and Clean Energy*, vol. 4, no. 1, pp. 76–86, 2016, https://doi.org/10.1007/s40565-015-0176-1.

[18] C. N. Rowe, T. J. Summers, and R. E. Betz, "Arctan power frequency droop for power electronics dominated microgrids," *Australian Journal of Electrical and Electronics Engineering*, vol. 10, no. 2, pp. 157–166, 2013, https://doi.org/10.7158/E12-012.2013.10.2.

[19] A. E. M. Bouzid, P. Sicard, H. Chaoui, A. Cheriti, M. Sechilariu, and J. M. Guerrero, "A novel Decoupled Trigonometric Saturated droop controller for power sharing in islanded low-voltage microgrids," *Electric Power Systems Research*, vol. 168, pp. 146–161, Nov. 2019, https://doi.org/10.1016/j.epsr.2018.11.016.

[20] S. J. Williamson, A. Griffo, B. H. Stark, and J. D. Booker, "A controller for single-phase parallel inverters in a variable-head pico-hydropower off-grid network," *Sustainable Energy, Grids and Networks*, vol. 5, pp. 114–124, Nov. 2016, https://doi.org/10.1016/j.segan.2015.11.006.

[21] J. D. D. Iyakaremye, G. N. Nyakoe, and C. W. Wekesa, "Evaluation of MPC-based arctan droop control strategy in islanded microgrid," *EAI Endorsed Transactions on Energy Web*, vol. 8, no. 35, Feb. 2021, Art. no. e13, https://doi.org/10.4108/eai.19-2-2021.168724.

[22] A. Khaledian and M. Aliakbar Golkar, "Analysis of droop control method in an autonomous microgrid," *Journal of Applied Research and Technology*, vol. 15, no. 4, pp. 371–377, 2017, https://doi.org/10.1016/j.jart.2017.03.004.

[23] E. Pathan *et al.*, "Virtual Impedance-based Decentralized Power Sharing Control of an Islanded AC Microgrid," *Engineering, Technology & Applied Science Research*, vol. 11, no. 1, pp. 6620–6625, Feb. 2021, https://doi.org/10.48084/etasr.3946.